

STUDY OF THE POSITION OF THE DOMAIN WALL PINNING CENTRES
WITHIN THE $\text{Co}_{70.3}\text{Fe}_{4.7}\text{Si}_{15}\text{B}_{10}$ AMORPHOUS RIBBONS

STJEPAN SABOLEK and STANISLAV ZRNČIĆ

*Department of Physics, Faculty of Science, P.O.Box 162, University of Zagreb, 10001
Zagreb, Croatia*

Dedicated to Professor Mladen Paić on the occasion of his 90th birthday

Received 25 May 1995

Revised manuscript received 29 September 1995

UDC 539.213

PACS 75.50.Kj, 75.60.-d, 75.60.Ch

Variations of the positions and strengths of the domain wall pinning centres within an amorphous $\text{Co}_{70.3}\text{Fe}_{4.7}\text{Si}_{15}\text{B}_{10}$ ribbon were studied by means of a model for the influence of the surface fields H_p on the process of magnetization of amorphous ribbons. The strongest pinning centres are situated close to the free surface of the ribbon and the strength of the pinning centres decreases towards its centre.

1. Introduction

Main contribution to the magnetization of amorphous ferromagnetic ribbons along their length is associated with the motion of the π -domain walls (DW) of the main domain structure (MDS) [1,2]. At low frequency of the magnetizing field H the coercive field H_c , and the hysteresis loss E (the area of the $M - H$ loop) arise due to the pinning of the DW's at the pinning centres which they encounter during their motion [3]. Because of this, the knowledge of the types of the pinning centres and their distributions within the ribbons are important, both for a

better understanding of the magnetization processes, and in order to develop new materials with better soft magnetic properties.

It is known that a direct current (DC, J_D) and alternating current (AC, J) affect the process of magnetization of amorphous ferromagnetic ribbons [4,5]. In particular J_D , shifts and changes the shape of the maxima of the dM/dt versus H curve [6]. This affects some parameters of the $M - H$ loop, such as H_c , the remanent magnetization M_r , the maximum permeability μ_{max} and in some cases the maximum magnetization M_m . Usually, J_D also shifts the center C of the $M - H$ loop [7]. A simple model that explains these effects in terms of the field H_p generated by J_D has been proposed [8]. A number of the experiments [8,9] proved the validity of the model.

AC (J) can produce $H_c = 0$ in some amorphous ribbons [10]. This phenomenon can also be explained in terms of the model developed for J_D [10]. It has been shown that large difference between the strengths of the pinning centres situated close to the opposite surfaces of the ribbon (ΔS) facilitates the achievement of $H_c = 0$.

Here we show how the model for the influence of H_p on the magnetization of amorphous ribbons enables the approximate determination of the positions of the DW pinning centres within the samples, and also the determination of the samples surface near which the pinning of the DW's is stronger. The knowledge which side of the ribbon accommodates the stronger pinning centres is important in a case when one wishes to increase or decrease artificially ΔS . (The increase of ΔS can then be used to achieve $H_c = 0$ by means of J).

2. Model

As previously described [6-10], we consider a hypothetical ribbon consisting of two domains separated by π -DW. The domain magnetizations I forms an angle δ with the ribbon axis. We label one surface of the ribbon as the "upper" and the opposite as the "lower" one. Accordingly, we denote the strengths of the pinning centres close to upper and lower surfaces of the sample by S_u and S_l , respectively, and, for the calculational purposes, we assume $S_u < S_l$. We also define the average pinning strength $\langle S \rangle = (S_l + S_u)/2$ and the pinning inhomogeneity $\Delta S = S_l - S_u$. The magnetizing field H , increasing from $-H_0$ to H_0 (H_0 is the field amplitude), is taken as "positive" ($H > 0$), whereas that decreasing from H_0 to $-H_0$ as "negative". The magnitude of H required to release DW in the absence of the core current from the upper and lower surface of the sample we denote by H_{su0} and H_{sl0} , respectively. The corresponding quantities, when the core current flows, are H_{su} and H_{sl} (for $H > 0$) and H_{su}^- and H_{sl}^- (for $H < 0$). The projection of the field H_p generated by the core current on I we denote by P . Clearly, depending on the direction of J_D , $P \neq 0$ results.

As shown earlier [9-11], when J_D flows along the ribbon, one finds

$$H_c = H_{c0}, \quad (1)$$

$$C = \mp H_p \tan \delta, \quad (2)$$

for $P \leq \Delta S/2$, and

$$H_c = \langle S \rangle / \cos \delta - H_p \tan \delta, \quad (3)$$

$$C = \mp \Delta S/2 \cos \delta, \quad (4)$$

for $P > \Delta S/2$. The signs in Eqs. (2) and (4) correspond to the two directions of J_D [9]. For thin long ribbon, $H_p = yJ_D/wt$, where w and t are width and thickness of the ribbon and y is the vertical distance from the centre of the ribbon ($-t/2 \leq y \leq t/2$) [5]. Therefore, for $P \leq \Delta S/2$, the centre C of the $M - H$ loop shifts linearly with J_D . The slope of the $C(J_D)$ variation is

$$\Delta C / \Delta J_D = y \tan \delta / \omega t. \quad (5)$$

This slope can provide the interesting information about the positions (y) from which DW's are released and about the angle δ . The diagrams showing the variations of H_c , C and the depinning field H_S of DW with $H_p(J_D)$ are shown in Fig. 1 of Ref. 9.

The surface field, H_p , can also be produced by external sources [11,12]. If such field acts at the upper surface of the sample only (inset to Fig. 1), the magnetizing fields required to release DW from the upper and lower surface of the ribbon, respectively, are

$$H_{su} = H_{su0} \mp H_p \tan \delta, \quad (6)$$

$$H_{sl} = H_{sl0}, \quad (7)$$

$$H_{su}^- = -H_{su0} \mp H_p \tan \delta, \quad (8)$$

$$H_{sl}^- = -H_{sl0}. \quad (9)$$

The upper signs in Eqs. (6) and (8) correspond to the direction H_p shown in the inset to Fig. 1, and the lower ones to the opposite direction of H_p . For H_p acting on the "lower" surface only follows:

$$H_{su} = H_{su0}, \quad (10)$$

$$H_{sl} = H_{sl0} \mp H_p \tan \delta, \quad (11)$$

$$H_{su}^- = -H_{su0}, \quad (12)$$

$$H_{sl}^- = -H_{sl0} \mp H_p \tan \delta. \quad (13)$$

According to the relations (6) to (13), H_c does not change with H_p for $P \leq \Delta S/2$ both for H_p acting at the "lower" and the "upper" surface of the sample. When H_p acts at the "upper" surface only, C obeys Eq. (4) and for H_p acting on the "lower" surface, $C = 0$, all for $P \leq \Delta S/2$.

For $P > \Delta S/2$, H_c decreases linearly with H_p both for H_p acting at the "upper" and "lower" surface only:

$$H_c = \langle S \rangle / \cos \delta - H_p \tan \delta/2. \tag{14}$$

Within the same regime for H_p acting at the "upper" surface only, one finds for C

$$C = \mp(\Delta S/2 \cos \delta + H_p \tan \delta/2). \tag{15}$$

The corresponding relation for H_p along the "lower" surface is

$$C = \mp(-\Delta S/2 \cos \delta + H_p \tan \delta/2). \tag{16}$$

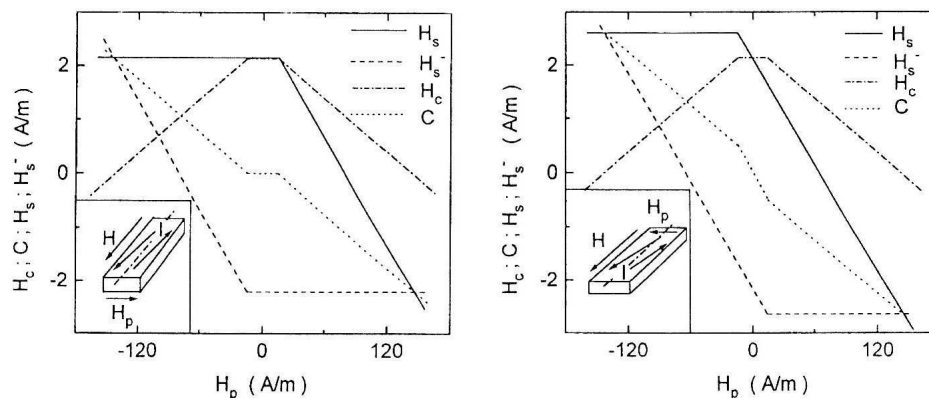


Fig. 1. Variations of the coercive field H_c , position of the centre of the $M - H$ loop C and depinning fields H_s and H_s^- (required in order to release DW's for the "positive" and "negative" H , respectively) with the surface field H_p for the case when H_p acts on the "upper" surface of the ribbon only. The inset: schematic representation of fields acting on the sample when H_p is applied to the "upper" surface only (I is the domain magnetization).

Fig. 2. Variations of the same quantities from Fig. 1 in a case when H_p acts at the lower surface only. The inset: schematic representation of the fields acting on a sample (right).

Graphical representation of the above relations is given in Figs. 1 and 2. Obviously, the measurements with an external H_p applied first to one and then to the other surface of the ribbon allows (by the use of the above relations) to determine which surface of the ribbon is closer to the stronger DW pinning centres.

3. Experimental

The investigation of the DW pinning centres has been performed on an amorphous nonmagnetostrictive $\text{Co}_{70.3}\text{Fe}_{4.7}\text{Si}_{15}\text{B}_{10}$ (hereafter CoFeSiB) alloy. All measurements were performed on the same sample in a form of ribbon with the dimensions $l \times w \times t = 200 \text{ mm} \times 2 \text{ mm} \times 0.02 \text{ mm}$. The magnetization measurements were performed using the induction technique [13] at room temperature. The triangular drive field H , with the frequency 5.5 Hz, has been used. In order to access the distribution of the strengths of the pinning centres dominating the process of magnetization in different ranges of M_m , the $M - H$ loops have been measured for different amplitudes H_0 of the drive field H . In order to determine the positions within the ribbon of the pinning centres governing the variations of the parameters of the $M - H$ loops for a given M_m , J_D has been passed along the sample during the magnetization measurements. In order to determine the surface of the ribbon exhibiting the stronger pinning of DW's, we used the combination of the homogeneous field H_z achieved with the Helmholtz pair of coils and the field H_i generated with the direct core current J_D , as illustrated in Fig. 3. Obviously, for the properly selected J_D , one achieves $|H_i| = |H_z|$, in which case the resultant field H_p is zero at one surface (lower in Fig. 3) of the ribbon. On the opposite surface, $H_p = H_i + H_z$. The profile of the magnetic field within the sample, which may be expected in this case is shown in the inset to Fig. 3.

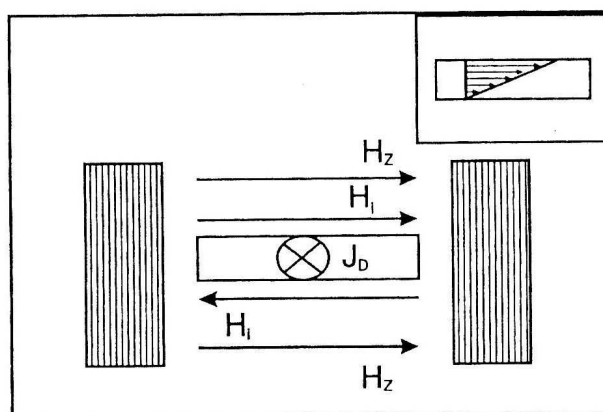


Fig. 3. Drawing illustrating the method for production of field acting on one surface of the sample ("upper") by using the combination of constant field H_z (generated by the Helmholtz coils) and field H_i generated by constant current J_D flowing along the sample. The inset: field profile within the sample.

4. Results

The variations of H_c and M_r with M_m/M_s (M_s is the saturation magnetization) for CoFeSiB sample in the absence of H_p are shown in Fig. 4. As reported in Ref.

14, both H_c and M_r show somewhat different variations in different ranges of M_m/M_s . In particular, H_c shows power law variations $H_c \sim (M_m/M_s)^\alpha$ with the exponent $\alpha \approx 0.15$ for $M_m/M_s \leq 0.5$, $\alpha \approx 1.1$ for $0.5 < M_m/M_s < 0.75$ and $\alpha \approx 6.4$ for $M_m/M_s > 0.75$, which agrees well with the earlier results for different samples of the same alloy [14]. The regions of M_m/M_s , corresponding to the values of $\alpha \approx 0.15, 1.1$ and 6.4 , are labeled with I, II and III, respectively, in Figs. 4 and 5. M_r also shows different variations in the same three regions of M_m/M_s (Fig. 4). In particular, the increase of M_r with M_m/M_s is slower in the region I, then in II and M_r tends to saturate in the region III.

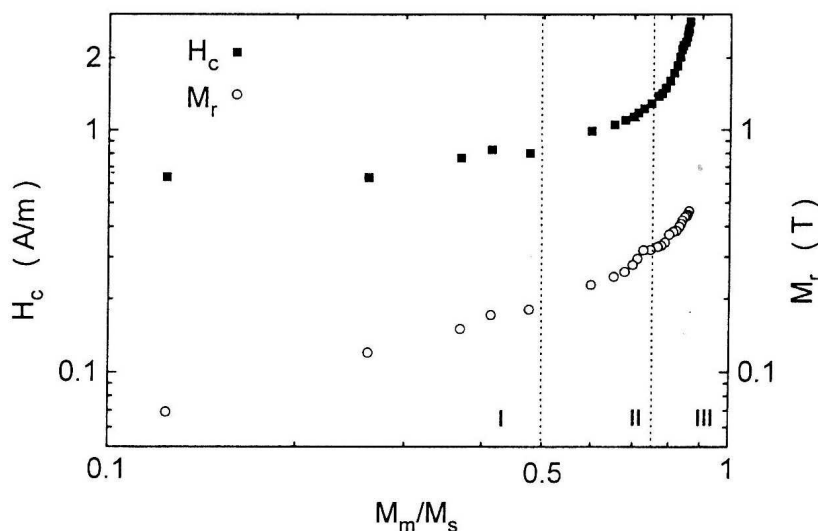


Fig. 4. Variations of the remanence M_r and coercive field H_c of $\text{Co}_{70.3}\text{Fe}_{4.7}\text{Si}_{15}\text{B}_{10}$ amorphous sample with maximum magnetization M_m normalized to the saturation magnetization M_s . Numbers I, II and III denote regions with different variations of H_c and M_r with M_m/M_s . The triangular drive field with frequency 5.5 Hz was employed.

The slopes of variation of C versus J_D (measured within the range of J_D values over which C varies linearly with J_D), $\Delta C/\Delta J_D$, initially increase with M_m but tend to saturate for $M_m/M_s > 0.75$ (Fig. 5). Comparing the variation of $\Delta C/\Delta J_D$ with M_m/M_s with that of H_c with M_m/M_s (Fig. 4), we note that in the region I $\Delta C/\Delta J_D$ increases rapidly with M_m and reaches the value of about 15 m^{-1} at the end of this region. The increase of $\Delta C/\Delta J_D$ is slower in the region II ($\Delta C/\Delta J_D \leq 21.5 \text{ m}^{-1}$) and $\Delta C/\Delta J_D$ seems to saturate in the region III at the value 22 m^{-1} . As illustrated in Fig. 6a, the variations of C with J_D remain linear. Moreover, both the variation of H_c with J_D (approximately constant) and C with J_D (linear) show that the measurements were performed in the conditions $P < \Delta S/2$.

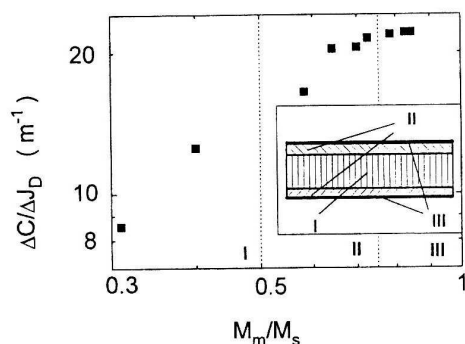


Fig. 5. The slope ($\Delta C/\Delta J_D$) of the variation of the position of $M-H$ loop centre C with the constant current J_D flowing through the $\text{Co}_{70.3}\text{Fe}_{4.7}\text{Si}_{15}\text{B}_{10}$ sample versus the normalized maximum magnetization M_m/M_s in different regions of M_m/M_s (denoted with I, II and III, respectively). The inset: illustration of the positions of the pinning centres effective in the regions I, II and III M_m/M_s . The frequency of the triangular drive field was 5.5 Hz.

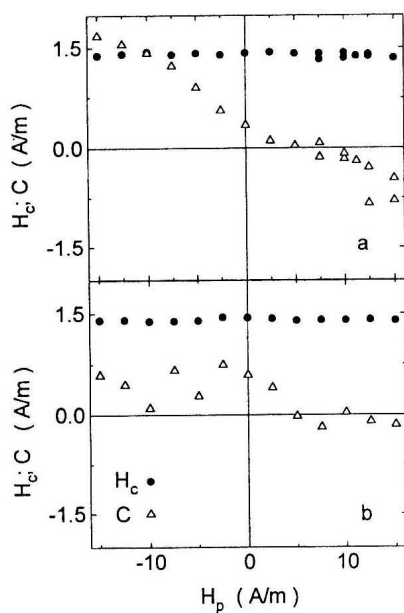


Fig. 6. Variation of the coercive field H_c (circles) and the position of the centre of the $M-H$ loop C (triangles) for $\text{Co}_{70.3}\text{Fe}_{4.7}\text{Si}_{15}\text{B}_{10}$ sample with: a) the field H_p generated by the direct core current J_D (open symbols), and H_p acting on "upper" surface only (solid symbols); b) the field H_p acting on "lower" surface only. The amplitude of the triangular magnetizing field was $H_0 = 25$ A/m and the frequency $f = 5.5$ Hz.

The results of the measurements performed with the field H_p at one surface of the ribbon only are shown in Fig. 6 with the solid symbols. Fig. 6a shows that for H_p applied at the upper surface only, C decreases linearly with H_p with the slope $\Delta C/\Delta H_p \approx 0.082$, which is close to that observed in a case of the core current J_D only. The total change of C within the employed interval of H_p is about 3.5 A/m, again essentially the same as in the case of J_D (giving approximately the same H_p) only. As shown in Fig. 6b, when H_p is applied at the lower surface of the ribbon only, C shows, within a considerable scatter of the data, only a weak variation with H_p . The total change of C within the same interval of H_p , as in Fig. 6a, is only about 0.75 A/m, which is about five times smaller than in a case of H_p applied at the upper surface only. The coercive field H_c is in both cases (H_p applied to the upper or lower surface only) approximately constant, which means, according to the model, that the condition $P < \Delta S/2$ is fulfilled.

5. Discussion

Several types of DW pinning centres (such as the structural defects in the magnetostrictive alloys, the intrinsic fluctuations in the exchange energy and local anisotropy, the surface defects (irregularities, the chemical inhomogeneities etc.) contribute to coercivity of amorphous ferromagnetics [3]. The different variations of M_r and H_c with M_m in the different regions M_m/M_s , observed both in the magnetostrictive and nonmagnetostrictive amorphous ferromagnets, indicate that different types of DW pinning centres dominate the process of magnetization in different regions of M_m/M_s . In particular, at lower M_m , the depinning of DW's from the weaker pinning centres is likely to dominate, whereas at elevated M_m , the stronger pinning centres seem to affect the magnetization of the sample [14]. Indeed a larger slope of the $\log H_c$ vs $\log(M_m/M_s)$ plot in Fig. 4 at elevated M_m indicates that the stronger pinning centres are effective at higher M_m [14]. The present (Fig. 4), as well as the earlier results [14], indicate that in the nonmagnetostrictive CoFeSiB alloys at least three types of pinning centres with different strengths can be associated with different dependences of M_r and H_c with M_m in three regions of M_m/M_s . As seen from Fig. 5, $\Delta C/\Delta J_D$ (which according to Eq. (6) depends both on the vertical distance of the pinning site from the centre of the ribbon and the angle δ) also shows different variations with M_m in the same three regions of M_m/M_s . Since the real samples possess a rather complex domain structure (i.e., different groups of domains form somewhat different angles δ with the ribbon axis [15]), we replace δ with an average value $\langle \delta \rangle$. For the rest of this discussion, we will assume that $\langle \delta \rangle$ does not change with M_m , hence $\Delta C/\Delta J_D$ depends on the distance y of effective pinning centres from the centre of the ribbon only. Clearly, the region III in Figs. 4 and 5 is associated with the strongest DW pinning centres. Since $\Delta C/\Delta J_D$ saturates in this region (Fig. 5), this probably indicates that these pinning centres are situated at the largest y , i.e., close to the surface of the ribbon ($y = t/2$). This conclusion is consistent with the earlier experiments in which the etching of the surfaces of the samples caused a rapid decrease of H_c [16]. Since $\Delta C/\Delta J_D$ is proportional to y for constant δ (Eq. (6)), we can determine the

approximate positions of the different pinning centres as illustrated in the inset to Fig. 5. By using Eq. (6), we estimate that the weakest DW pinning centres (region I in Fig. 4) are situated in the interior of the ribbon within about $9\mu\text{m}$ from its centre, whereas the stronger ones (corresponding to region II in Fig. 4) are at larger distances y . Obviously, the borderlines between the different regions are not sharp, because in the real sample there should exist some distributions in the pinning strengths and, hence, some kind of gradual change in the average pinning strength on going from the centre towards the surface of the sample. The strongest pinning centres are, however, situated close to the sample surface and can, therefore, be associated with the surface irregularities and inhomogeneities [3].

In the model for the influence of H_p on the magnetization of amorphous ribbons we assumed the different pinning strengths at the opposite surfaces of the ribbon ($\Delta S \neq 0$). Indeed, during the production of the amorphous ribbons (melt-spinning), one side of the ribbon is in the contact with the roller ("contact" surface) whereas the other is free ("free" one). Because of this, the surface irregularities (and presumably the inhomogeneities) are different on the two surfaces, which leads to different pinning of DW's [3]. The different variations of C with H_p (Fig. 6) for H_p on the "contact" and "free" surface of the ribbon, respectively, support the different pinning of DW's at the two surfaces. (In our experiments the "contact" surface was the "upper" one and the "free" surface was "lower" one). In particular, a linear change of C with H_p for H_p acting on the "contact" ("upper") surface shows, according to Eq. (4) that the pinning centres at this surface are weaker than those at the "free" surface. Conversely, a weak irregular change of C with H_p acting on the "free" ("lower") surface is consistent with the stronger pinning of DW's at this surface.

6. Conclusion

The detailed measurements of the magnetization of the amorphous ferromagnetic CoFeSiB ribbon have shown that the strongest DW pinning centres are situated in the immediate vicinity of the surface of the ribbon and that the strength of the pinning centres decreases towards the centre of the ribbon. The calculation shows that the model for the influence of the "surface" field H_p on the process of magnetization of amorphous ribbons can be used for the approximate determination of the positions of the different DW pinning centres within the ribbon.

In addition, the model has been extended to the case in which H_p acts on one surface of the sample only. Depending whether H_p acts on the surface of the sample containing stronger or weaker DW pinning centres, a different variation of C with H_p is predicted. This finding enabled us to show that in the employed as-prepared non magnetostrictive CoFeSiB alloy, the stronger pinning centres are situated at the "free" surface of the ribbon. The method employed in this paper is non-destructive and can be employed for any kind of amorphous or conventional ferromagnets in a form of a ribbon. This is important because the effects of the various surface treatments aimed for the improvement of the magnetic properties of these materials can be easily monitored.

References

- 1) Y. Obi, H. Fujimori and H. Saito, J. Appl. Phys. **15** (1976) 611;
- 2) P. Schönhuber, H. Pfützner, G. Harasko, T. Klinger and K. Futschik, J. Magn. Magn. Mater. **112** (1992) 349;
- 3) H. Kronmüller, J. Magn. Magn. Mater. **24** (1981) 159;
- 4) C. Aroca, E. Lopez and P. S. Sanchez, J. Magn. Magn. Mater. **92** (1981) 159;
- 5) R. N. G. Dalpadado, IEEE Trans. Magn. MAG-17 (1981) 3163;
- 6) J. Horvat and E. Babić, J. Magn. Magn. Mater. **92** (1990) 25;
- 7) J. Horvat, phys. stat. sol. (a) **134** (1992) 521;
- 8) J. Horvat, phys. stat. sol. (a) **129** (1992) 519;
- 9) S. Sabolek, E. Babić and K. Zadro, Fizika A1 (1992) 167;
- 10) S. Sabolek, E. Babić and Ž. Marohnić, Phys. Rev. B **48** (1993) 6206;
- 11) J. Horvat, E. Babić and G. J. Morgan, J. Magn. Magn. Mater. **104** (1985) 359;
- 12) S. Sabolek, J. Horvat, E. Babić, and K. Zadro, J. Magn. Magn. Mater. **110** (1992) 25;
- 13) J. Horvat, Ž. Marohnić and E. Babić, J. Magn. Magn. Mater. **82** (1989) 5;
- 14) J. Horvat, E. Babić, Ž. Marohnić and H. H. Liebermann, J. Magn. Magn. Mater. **87** (1990) 339;
- 15) H. J. de Wit and M. Brouha, J. Appl. Phys. **57** (1985) 3560;
- 16) J. J. Becker, J. Appl. Phys. **52** (1981) 1905.

PROUČAVANJE POLOŽAJA CENTARA ZAPINJANJA DOMENSKIH
ZIDOVA U AMORFNOJ $\text{Co}_{70.3}\text{Fe}_{4.7}\text{Si}_{15}\text{B}_{10}$ VRPCI

Korištenjem modela za utjecaj površinskih polja H_p na proces magnetiziranja amorfnih feromagnetskih vrpca proučavan je položaj i jakost centara zapinjanja unutar amorfne $\text{Co}_{70.3}\text{Fe}_{4.7}\text{Si}_{15}\text{B}_{10}$ vrpce. Rezultati mjerenja, dobiveni djelovanjem polja H_p samo na jednoj površini, pokazuju da se jači centri zapinjanja nalaze na površini koja u procesu proizvodnje nije bila u kontaktu s valjkom. Ta činjenica je važna za daljnje tretiranje uzorka radi poboljšanja mekih magnetskih svojstava amorfnih feromagnetskih vrpca.